Available online at www.sciencedirect.com
ScienceDirect
Journal of Solid State Chemistry 179 (2006) 3107–3113
JOURNAL OF SOLID STATE CHEMISTRY
www.elsevier.com/locate/jssc

The crystal structure, thermal behaviour and ionic conductivity of a novel lithium gadolinium polyphosphate $LiGd(PO_3)_4$

Hasna Ettis, Houcine Naïli*, Tahar Mhiri

Laboratoire de l'Etat Solide (L.E.S), Université de Sfax, Faculté des Sciences de Sfax, 3018 Sfax, Tunisia

Received 10 April 2006; received in revised form 4 June 2006; accepted 4 June 2006
Available online 13 June 2006

Abstract

Crystal structure and ionic conductivity of lithium gadolinium polyphosphate, $LiGd(PO_3)_4$, were investigated. Single crystals of the title compound have been grown by a flux technique. The structure of this novel phosphate was determined by single crystal X-ray diffraction techniques. $LiGd(PO_3)_4$ is isotypic with $LiNd(PO_3)_4$. It crystallizes in the monoclinic space group $C2/c$ with the unit cell parameters $a = 16.386(2)$, $b = 7.059(3)$, $c = 9.677(2)$ Å, $\beta = 126.12(1)^\circ$, $V = 904.2(4)$ Å^3 and $Z = 4$. The structure refined from 967 independent reflections leads to $R_1 = 0.0167$ and $wR_2 = 0.0458$. The lattice of $LiGd(PO_3)_4$ is built of twisted zig–zag chains running along with the b direction and make up of PO_4 tetrahedra sharing two corners, connected to the GdO_8 and LiO_4 polyhedra by common oxygen atoms to form a three-dimensional framework. Differential and thermogravimetric thermal analysis are given. The thermal curve of this compound was recorded and interpreted in agreement with impedance measurements. The ionic conductivity has been measured on pellet of the polycrystalline powder and evaluated as a function of temperature. This phase showed the conductivity of 2×10^{-6} and $2 \times 10^{-4}\,\Omega^{-1}\,cm^{-1}$ at 682 and 951 K, respectively.

Keywords: Inorganic compounds; Impedance spectroscopy; X-ray diffraction; Crystal structure; Ionic conductivity

1. Introduction

There is a growing interest in the growth and characterization of various phosphates with the beginning of their applications as laser materials [1–7]. Alkali lanthanide phosphates were extensively studied owing to their wide applications in electricity, catalysis and due to their interesting optical properties [8–12]. Such compounds were mainly reported as cyclo and polyphosphates [13–15]. These condensed phosphates, synthesized by the flux method, are less easier to obtain in the form of single crystals with high quality. The literature dealing with these compounds is currently well established. In fact, the $M^IM^{III}(PO_3)_4$, (based chain structure), compounds can be classified into seven different structural types, nowadays usually denoted by roman numerols I–VII. This nomenclature first proposed by Palkina et al. [16] is today generally accepted. Previous structure analyses have shown that the inorganic phosphates with general formula $M^IM^{III}P_4O_{12}$ (M^I = alkali metal, M^{III} = rare earth metal; based cyclic structure) crystallize in two systems: cubic with $I\text{-}43d$ space group and monoclinic with $C2/c$ space group. Hence considerable interest of research into systems containing monovalent and trivalent cation long chain (or cyclic) phosphates as a possible basis for productive inorganic materials. In addition, many of these compounds are isotropic and some of them are polymorphic. Moreover, these types of phosphates with cyclic or chain geometry are stable under normal conditions of temperature and moisture and form all glasses after melting [17]. Here, we report a new condensed phosphate compound. However, to our knowledge, the crystal structure and properties of phosphates containing gadolinium in combination with lithium are not described in the $M^IM^{III}(PO_3)_4$ family. In order to find new materials with optimal properties and to enrich the chemistry of inorganic phosphates, we successfully synthesized the solid-state compound $LiGd(PO_3)_4$ (type I) in our laboratory. The present work deals with preparation and the single-crystal

*Corresponding author. Tel.: +216 74 27 49 23; fax: +216 74 274 437.
E-mail address: houcine_naili@yahoo.com (H. Naïli).

0022-4596/$ - see front matter © 2006 Elsevier Inc. All rights reserved.
doi:10.1016/j.jssc.2006.06.003

determination of the title compound. Furthermore, the thermal behaviour and the ionic conductivity measurements of this sample were performed.

2. Experimental procedure

2.1. Synthesis

The single-crystals of $LiGd(PO_3)_4$ were grown from Li_2O–Gd_2O_3–P_2O_5 melt. In the first stage of preparation, the initial mixture of Li_2CO_3, $NH_4H_2PO_4$ and Gd_2O_3 in a molar ratio of 15:75:6 was progressively heated in air up to 473 K for reaching decomposition of the phosphate and carbonate. All chemicals were commercial products of reagent grade, used without future purification. The resulting Li_2O–Gd_2O_3–P_2O_5 melt was heated in a platinium crucible at 1223 K over night. The temperature was then reduced at a rate of 2 K/h to 973 K and the furnace power turned off. The obtained $LiGd(PO_3)_4$ single crystals were leached from the remaining oxide Gd_2O_3 with boiling water and with nitric acid. Colourless, transparent and parallelepiped-shaped crystals obtained by this procedure are suitable for X-ray analysis. The formula of this compound is determined by chemical analysis (Table 1) and confirmed by refinement of the crystal structure.

2.2. Structure refinement

A colourless, parallelepipedic and single crystal of $LiGd(PO_3)_4$ with approximate dimensions of $0.18 \times 0.25 \times 0.28\,mm^3$ was selected for X-ray diffraction determination. The diffraction data were collected on an Enraf Nonius CAD-4 automated four-circle diffractometer with graphite-monochromated MoK_α radiation ($\lambda = 0.71073$ Å) using the $\omega/2\theta$ scan mode at the room temperature. An empirical absorption correction was applied using psi-scan method [18]. The structure of the title compound was solved using the Patterson heavy atom function and refined on F^2 by full-matrix least-squares method. The cell parameters obtained from single-crystal diffractometer measurements are: $a = 16.386(2)$, $b = 7.059(3)$, $c = 9.677(2)$ Å and $\beta = 126.12(1)^\circ$ with $C2/c$ space group. 981 reflections were collected in the quarter of Ewald sphere for $3.08 \leqslant \theta \leqslant 26.96$, of which 967 reflections had an intensity $I > 2\sigma(I)$. The structure was successfully developed in the centrosymetric $C2/c$ space group. Gadolinium and phosphorus atom positions were located using SHELXS-97 program [19], whereas lithium and oxygen atom positions were deduced from difference Fourier maps during the refinement of the structure with an adopted version of SHELXL-97 program [20]. When all the atoms were anisotropilly refined, the agreement factors R_1 and wR_2 converged, respectively, to 0.0167 and 0.0458. The chemical crystal data, the parameters used for the X-ray diffraction data collection and the results of crystal structure determination of $LiGd(PO_3)_4$ are listed in Table 2. The final fractional atomic coordinates and the

Table 1
Results of chemical analysis for $LiGd(PO_3)_4$

	P (%)	Li (%)	Gd (%)
Calculated	25.8	1.44	32.75
Experimental	24.45[a]	1.72[b]	32.52[b]

[a]Determined by spectrophotometry.
[b]Determined by ICP method.

Table 2
Crystal data and structure refinement for $LiGd(PO_3)_4$

Crystal data	
Empirical formula	$LiGd(PO_3)_4$
Crystal system	Monoclinic
Space group	$C2/c$
Z	4
Temperature (K)	293(2)
Formula weight ($g\,mol^{-1}$)	480.07
Unit cell dimensions	
a (Å)	16.386(2)
b (Å)	7.059(3)
c (Å)	9.677(2)
β (°)	126.12(1)
Volume (Å^3)	904.2(4)
D_x	3.527
$F(0\,0\,0)$	892
Data collection	
Radiation	Mo$K\alpha$ ($\lambda = 0.71073$ Å)
Monochromator	Graphite
Diffractometer: Enraf- Nonius	CAD-4
Absorption coefficient (mm^{-1})	8.110
θ range (°)	3.08–26.96
Index ranges	$-20 < h < 16$ $0 < k < 8$ $0 < l < 12$
Scan type	ω–2θ
Reflections collected [$I > 2\sigma(I)$]	981
Independent reflections [$I > 2\sigma(I)$]	967
Refinement	
Refinement method	Full-matrix L.S. on F^2
Parameters refined	84
Weighting scheme	$\omega = 1/[\sigma^2(F_0^2) + (\alpha P) + \beta P]$, where $P = (F_0^2 + 2F_c^2)/3$
α	0.0294
β	8.04
Absorption correction	
ψ scan[18]	
T_{min}	0.1262
T_{max}	0.2303
Extinction coefficient	0.0145(5)
Goodness-of-fit	1.016
Final R indices [$I > 2\sigma(I)$]	
R_1	0.0167
wR_2	0.0458
Maximum shift/ESD	0.000
Mean shift/ESD	0.000
Largest diff. peak and hole (e Å^{-3})	1.12; −0.83 (near Gd atom)

$R_1 = (\Sigma[|F_0| - |F_c|]/\Sigma|F_0|$ $wR_2 = (\Sigma[W(F_0^2 - F_c^2)^2]/[W(F_0^2)^2])^{1/2}$.

selected bond lengths and angles are given in Tables 3 and 4, respectively.

2.3. Complex impedance techniques

Ionic conductivity of $LiGd(PO_3)_4$ was determined by employing ac impedance measurements. Specimen for the conductivity measurements was prepared from powder sample by pressing it into disk with 13 mm in diameter and 1 mm in thickness ($P = 62$ bar and $D = 0.145$). The compactness of obtained sample is about 90%. On both sides of the disk surface, silver was deposited to form thin films as blocking electrodes. To avoid the influence of moisture, the specimen was dried at 100 °C before measurements. The ac impedance measurements were made using HP 4192A impedance analyzer in the range from 5 to 13 MHz and measurements were carried out in vacuum over thermal intervals 293–951 K. The sample was maintained few minutes at each temperature before collecting data; the temperature stability was ±1 K.

3. Results and discussion

3.1. Description of the structure

Projection on ac plane is depicted in Fig. 1. As a result of our investigations, $LiGd(PO_3)_4$ was shown to be isostructural with $LiNd(PO_3)_4$ [22]. From a general point of view, this phosphate could be described as a long chain polyphosphate organisation containing an alternating zigzag chains $(PO_3)_n$ and (Gd^{3+}, Li^+) cations along the *b* direction. The structure can be regarded also as being made of anionic and cationic sheets advancing along the [0 0 1] direction as shown in Fig. 1. The cationic layers are located between these sheets; interaction between oxygen and (Gd^{3+}, Li^+) cations ensure the cohesion of the structure (Fig. 1). The basic structure units of $LiGd(PO_3)_4$ are two meandering chains formed by corner-sharing PO_4 tetrahedra with the $(PO_3)^-$ formula. The chains $(PO_3)^-_n$ (two per unit cell) run along *b* direction. These chains are joined

Table 3
Fractional atomic coordinates and temperature factors for $LiGd(PO_3)_4$

Atoms	*x*	*y*	*z*	$U_{éq}$
Gd	0.0000	0.29794(3)	0.7500	0.00403(13)
Li	0.0000	−0.2037(12)	0.7500	0.0112(18)
P(1)	−0.13805(6)	0.05352(12)	0.33843(11)	0.00446(19)
P(2)	−0.14755(6)	−0.34718(13)	0.40305(11)	0.00457(19)
O(L12)	−0.15828(19)	−0.1235(4)	0.4168(3)	0.0083(5)
O(L21)	−0.24438(18)	0.0810(4)	0.1563(3)	0.0080(5)
O(E21)	−0.07225(19)	−0.4106(4)	0.5834(3)	0.0091(5)
O(E11)	−0.1138(2)	0.2172(4)	0.4539(3)	0.0093(5)
O(E22)	−0.12912(19)	−0.3856(4)	0.2721(3)	0.0097(5)
O(E12)	−0.06534(18)	0.0029(4)	0.2973(3)	0.0079(5)

Estimated standard deviations are given in parentheses. $U_{éq} = 1/3\sum_i\sum_j U_{ij}a_i^*a_j^*a_ia_j$.

Table 4
Atomic distances (Å) and angles (°) in $LiGd(PO_3)_4$ with standard deviations in parentheses

Tetrahedra around P(1)					
P(1)–O(E11)	1.490(3)	O(E11)–O(E12)	2.576(4)	O(E11)–P(1)–O(E12)	118.7(1)
P(1)–O(E12)	1.505(3)	O(E11)–O(L12)	2.478(4)	O(E11)–P(1)–O(L12)	106.8(1)
P(1)–O(L12)	1.595(3)	O(E11)–O(L21)	2.556(4)	O(E12)–P(1)–O(L12)	111.0(1)
P(1)–O(L21)	1.600(2)	O(E12)–O(L12)	2.555(4)	O(E11)–P(1)–O(L21)	111.6(1)
		O(E12)–O(L21)	2.461(3)	O(E12)–P(1)–O(L21)	104.8(1)
		O(L12)–O(L21)	2.497(4)	O(L12)–P(1)–O(L21)	102.8(1)
Tetrahedra around P(2)					
P(2)–O(E22)	1.490(3)	O(E22)–O(E21)	2.582(4)	O(E22)–P(2)–O(E21)	119.8(1)
P(2)–O(E21)	1.493(3)	O(E22)–O(L21)^{V}	2.554(4)	O(E22)–P(2)–O(L21)^{V}	112.1(1)
P(2)–O(L21)^{V}	1.589(2)	O(E22)–O(L12)	2.530(4)	O(E21)–P(2)–O(L21)^{V}	107.7(1)
P(2)–O(L12)	1.603(3)	O(E21)–O(L21)^{V}	2.489(3)	O(E22)–P(2)–O(L12)	109.7(1)
		O(E21)–O(L12)	2.452(4)	O(E21)–P(2)–O(L12)	104.7(1)
		O(L21)^{V}–O(L12)	2.463(4)	O(L21)^{V}–P(2)–O(L12)	101.0(1)
P(1)–P(2)^{V}	2.935(1)	P(1)^{V}–P(2)–P(1)	104.5(3)	P(1)–O(L12)–P(2)	132.0(2)
P(2)–P(1)	2.921(1)	P(2)–P(1)–P(2)^{V}	102.2(3)	P(1)–O(L21)–P(2)	134.1(2)
Polyhedra around Gd		*Tetrahedra around Li*			
Gd–O(E22)^{I}	2.332(3)	Li–O(E21)	1.970(7)	Li–Li^{I}	5.629(3)
Gd–O(E22)^{III}	2.332(3)	Li–O(E21)^{IV}	1.970(7)	Gd–Gd^{VII}	5.617(3)
Gd–O(E11)	2.390(3)	Li–O(E12)^{I}	1.986(7)	Gd–Li^{II}	3.518(1)
Gd–O(E11)^{IV}	2.390(3)	Li–O(E12)^{III}	1.986(7)		
Gd–O(E21)^{VI}	2.446(3)				
Gd–O(E21)^{II}	2.446(3)				
Gd–O(E12)^{I}	2.538(3)				
Gd–O(E12)^{III}	2.538(3)				

Symmetry code: I: $-x, -y, -z+1$; II: $x, y+1, z$; III: $x, -y, z+1/2$; IV: $-x, y, -z+3/2$; V: $-x-1/2, y-1/2, -z+1/2$; VI: $-x, y+1, -z+3/2$; VII: $-x, 1-y, 1-z$.

to one another by gadolinium and lithium polyhedra forming a three-dimensional framework (Fig. 2). By examining Fig. 3, we remark that the Gd^{3+} and Li^{+} ions alternated on twofold axes in the middle of four such chains. GdO_8 dodecahedra and considerably distorted LiO_4 tetrahedra form linear sharing their edges.

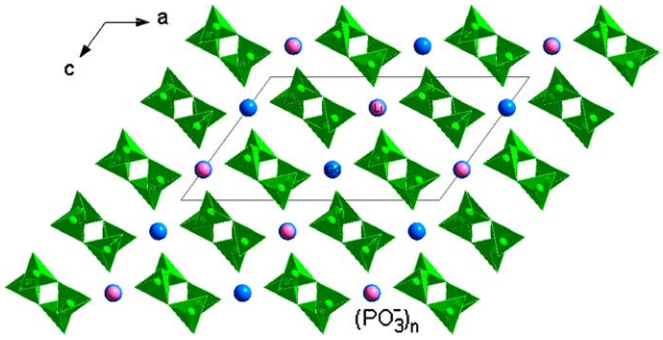

Fig. 1. Projection in ac plane of the $LiGd(PO_3)_4$ structure.

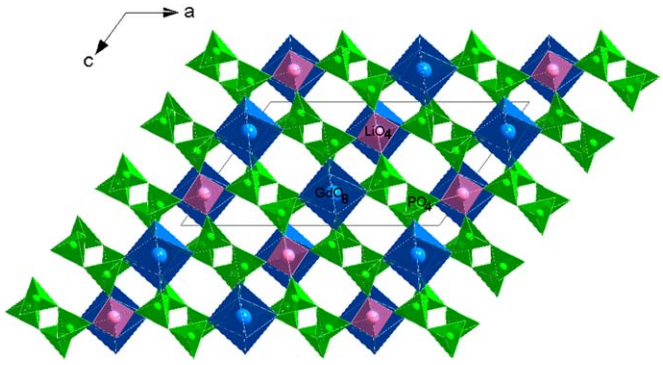

Fig. 2. The structural arrangement of the title compound viewed in the (0 1 0) plane.

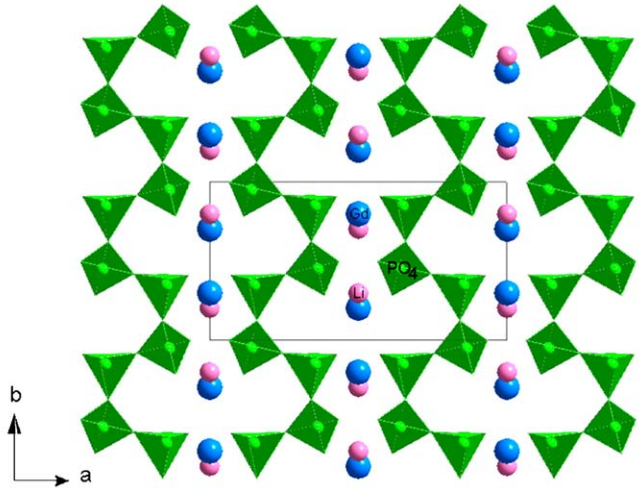

Fig. 3. [0 0 1] projection of the $LiGd(PO_3)_4$.

3.1.1. Phosphoric group

The helical arrangement of the corner-shared PO_4 tetrahedra chains can be clearly shown on [0 0 1] projection (Fig. 3). The asymmetric unit contains two crystallographically independent $(PO_3)^-$ groups. Each PO_4 tetrahedra is connected by two common corners in *cis* position to other PO_4 tetrahedra going rise to a twisted chain of general formula $(PO_3)^-_n$. These spiral chains with a period of four tetrahedra arranged around the 2_1 helical axe, parallel to the *b* direction. The main interatomic distances and bond angles are given in Table 4. The P–O distances can be divided into linking or bridging P–OL_{ij} and exterior P–OE_{ij} distances [where OL_{ij} denotes the oxygen atom links atom P_i with atom P_j, and OE_{ij} denotes the *j*th oxygen atom exterior to the chain and bonded to atom P_i [21]]. The linking distances, P–OL_{ij}, which range from 1.589(2) to 1.603(3) Å, are longer than the P–OE_{ij} distances, which vary from 1.490(3) to 1.505(3) Å. The P–O–P angles are understood between 132.0(2) and 134.1(2)°. Furthermore, three different types of O–P–O angles co-exist in the PO_4 tetrahedra. The O(L)–P–O(L) angles (mean value 101.9(1)°) correspond to the longest P–O bonds, the O(L)–P–O(E) angles have the value expected for a regular tetrahedron and the O(E)–P–O(E) angles correspond to the shortest P–O distances (mean value 119.2(1)°), probably induced by mutual repulsion of the non-bridging oxygen atoms. These results are in good agreement with those usually met in polyphosphates anions [6,22,23].

3.1.2. Gadolinium coordination

In the $LiGd(PO_3)_4$, the gadolinium atoms are eight-coordinated as shown in Fig. 4(a). The GdO_8 dodecahedra are considerably distorted. The Gd–O distances range between 2.332(3) and 2.538(3) Å (Table 4) with a mean value of 2.426(3) Å, in agreement with those met in the $MGd(PO_3)_4$ family ($M = K$ and Cs) which have been synthesized in our laboratory [13–15]. The GdO_8 dodecahedra share all their oxygen atoms with the corners and edges of neighbouring PO_4 and LiO_4 tetrahedra respectively. It is to be noted that the adjacent polyhedra do not share any oxygen atoms among them. The shortest Gd–Gd distance 5.617(3) Å is an intermediate value of those in $LiEr(PO_3)_4$ (5.567(1) Å) [24] and $LiNd(PO_3)_4$ (5.644 Å) [7]. This fact is due to the difference of the ionic radii between the rare earth cations where $r(Nd^{3+}) > r(Gd^{3+}) > r(Er^{3+})$.

3.1.3. Lithium coordination

The lithium cations are surrounded by four oxygen atoms (Fig. 4(b)). This environment is considerably irregular as can be seen in other lithium polytetraphosphates [7,22]. In fact, the Li–O distances vary from 1.970(7) to 1.986(7) Å with an average of 1.978(7) Å. The lithium tetrahedra are connected by common corners to $(PO_3)_n$ chains and by a common edges to gadolinium dodecahedra with a Gd–Li distance of 3.518(1) Å as shown in Fig. 4(c). With a comparison of the coordination number around Cs^+, K^+ and Na^+ in the structures of

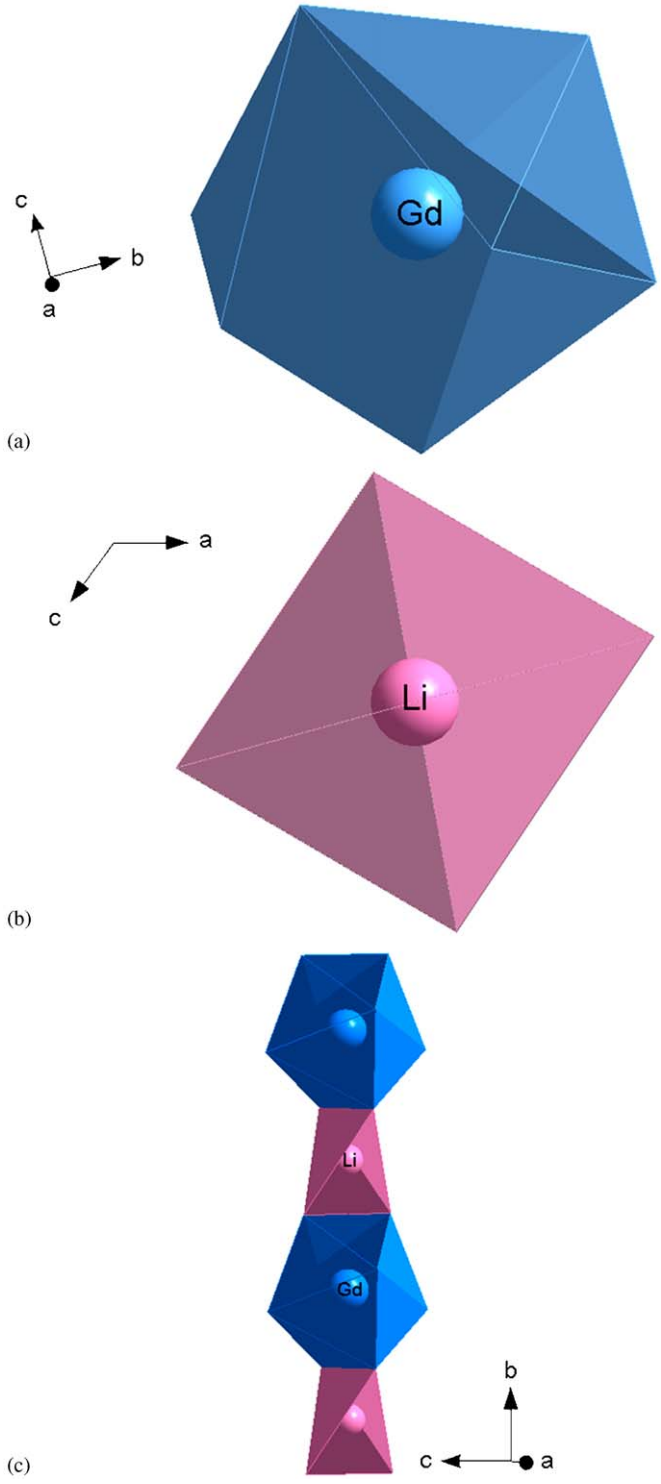

Fig. 4. (a) The O-atom coordination around the Gd atom, (b) the O-atom coordination around the Li atom, and (c) projection of an isolated chain of LiO_4 and GdO_8 polyhedra as observed in $LiGd(PO_3)_4$.

$CsGd(PO_3)_4$ [15], $KGd(PO_3)_4$ [14] and $NaNd(PO_3)_4$ [23], respectively, one can concluded that this number decreases from 11 for CsO_{11} polyhedra in the first compound to nine for the potassium (KO_9) and six for the sodium atom (NaO_6) in the second and the third materials, respectively, with only four for LiO_4 tetrahedra in the title compound. This result can be explained on the basis of the radii of the monovalent cations as $r(Cs^+)>r(K^+)>r(Na^+)>r(Li^+)$, so as the number of oxygens per cation in the chemical formula is constant, it is clear that one passes from a compact framework sharing all corners in $CsGd(PO_3)_4$ and $KGd(PO_3)_4$, to an open structure of coordination tetrahedra sharing only some edges in $LiGd(PO_3)_4$.

3.2. Thermal behaviour

Thermal analysis was performed using a RIGAKU Differential Thermal Analyzer operating from room temperature up to 1000 °C at an average rate of 5 °C min^{-1}. Calorimetric measurements were achieved between 50 and 1000 °C on a Mettler TA 4000 differential scanning calorimeter under the following conditions: heating rate of 5 °C min^{-1}, sample weight of 21.9 mg and sensitivity of 10 μV mW^{-1}. The two curves corresponding to the TGA and DTA analyses in air atmosphere of $LiGd(PO_3)_4$ are shown in Fig. 5. The DTA curve shows that the polyphosphate undertakes succession endothermic phenomena. Three endothermic peaks at 602, 640 and 971 °C are shown. The first and second peaks may be denoting structural phase transitions. The calculated transition enthalpy, for the first transition at $T_1 = 602$ °C, were $\Delta H_1 = 6.8\,Jg^{-1}$ and for the second transition at $T_2 = 640$ °C, $\Delta H_2 = 11.7\,Jg^{-1}$. The last peak at 971 °C corresponds to the decomposition of the product, which occurs with an enthalpy change $\Delta H_3 = 68\,J\,g^{-1}$. These results were well confirmed by the differential scanning calorimetry curve which shows that the title compound undertakes at about 605, 644 and 971 °C the same endothermic peaks. It is to be noted that the small obvious gain of mass which is observed in the TG curve (Fig. 5) is owed to the variation of the Archimedes push on the crucible and the carry sample.

3.3. Impedance spectroscopy analysis

Ionic conductivity measurements of the crystalline $LiGd(PO_3)_4$ phase were carried out. Some complex impedance diagrams ($-Z''$) versus (Z') recorded at various

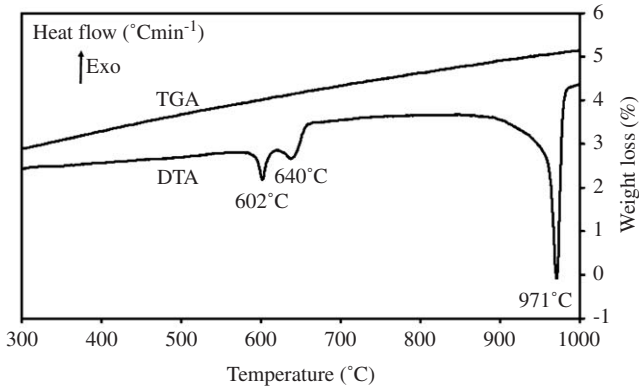

Fig. 5. DTA and TGA curves for $LiGd(PO_3)_4$.

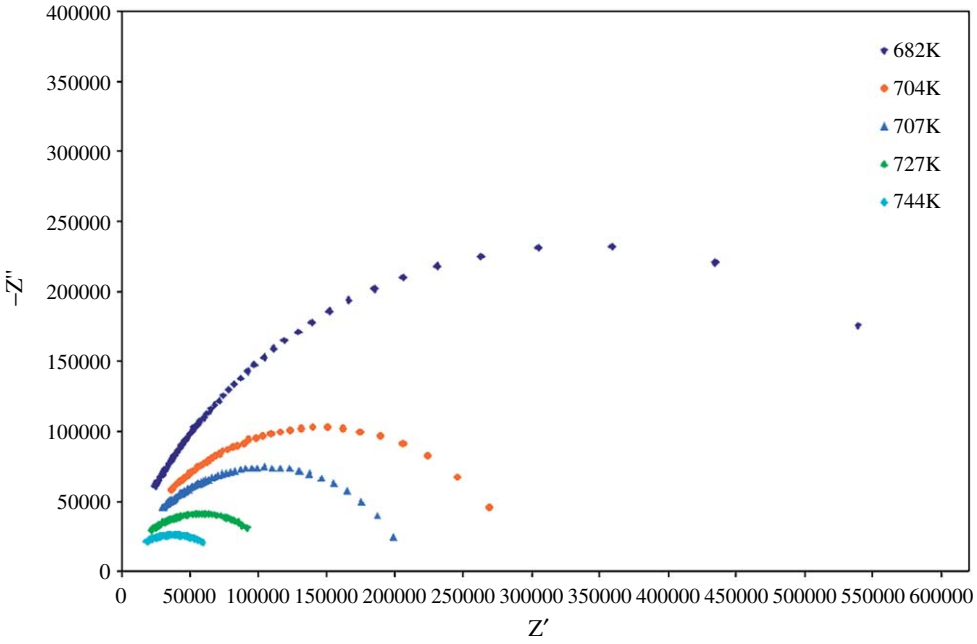

Fig. 6. Complex impedance diagrams $-Z'' =$ versus Z' for $LiGd(PO_3)_4$ at various temperatures.

temperatures are given in Fig. 6. The bulk ohmic resistance relative to the experimental temperature is the intercept on the real axis of the zero-phase angle extrapolation of the highest frequency curve. The parameter α represents the tilting angle ($\alpha\Pi/2$) of the circular arc from the real axis in the complex permittivity plane, is equal to 0.2. This angle represents the difference between the Cole–Cole and Debye law and is constant when the temperature various for all given impedance curve. Theses curves show the temperature dependence of the resistance proving a remarkable improvement of the ionic conduction of $LiGd(PO_3)_4$ material at high temperature which increases from $2\times10^{-6}\,\Omega^{-1}\,cm^{-1}$ at 682 K to $2\times10^{-4}\,\Omega^{-1}\,cm^{-1}$ at 951 K. The evolution of the conductivity versus reciprocal temperature $\log(\sigma T) = f(10^3/T)$ of the title compound is given in Fig. 7. This phase was found to have two breaks in the curve. An Arrhenius-type behaviour $\sigma T = \sigma_0 \exp(-E_a/kT)$ is shown. There are three distinct domains seen for the variation of $\log(\sigma T)$ with temperature. Each domain is seen as a linear segment which follows the Arrhenius law. Transitions between domains are seen at 725 and 873 K. The existence of the two domains around 725 K is not due to a first order phase change. In fact, differential thermal analysis and differential scanning calorimetry have shown the absence of such a change at this temperature. Thus, the existence of this break may be attributed to the presence of two types of conductivities: parallel to c axis (σc) and along the [1 0 1] direction (σac). These two different conductivities can be related to the resulting interaction between the $(PO_3)_n$ chains and the cationic layers along the [0 0 1] and [1 0 1] directions (Fig. 2). σc may be higher than σac since the Li–Li distance parallel to c axis (6.405(3) Å) is shorter than that calculated along the [1 0 1] direction (6.652(3) Å).

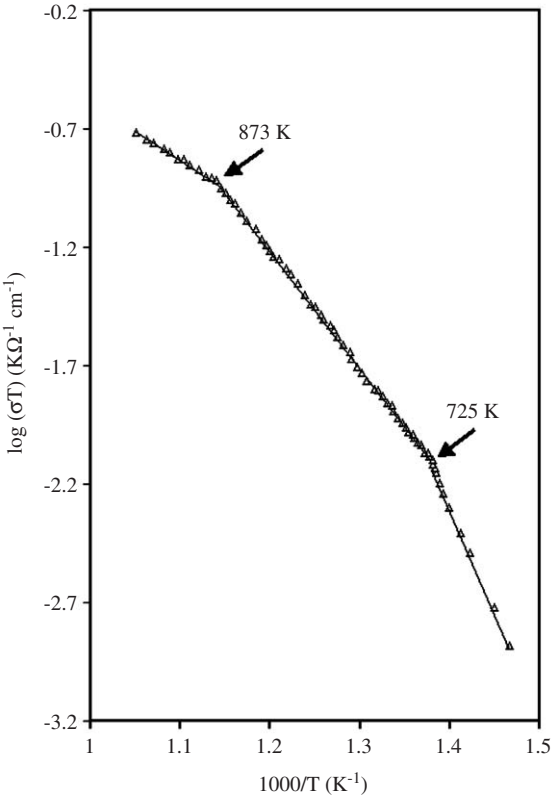

Fig. 7. Conductivity plots $\log(\sigma T) = f(10^3/T)$ for $LiGd(PO_3)_4$.

The last break can be attributed to the existence of two phase transitions above 873 K as confirm the DTA and DSC thermogrames. The activation energies calculated from Arrhenius plots are found to be temperature

depending. Their values are 1.7, 0.96 and 0.47 eV, respectively. The title compound shows a continuous and progressive increasing of the ionic conductivity by comparison with the $AgGd(PO_3)_4$ material (Naïli et al. in press) which showed a quite low ionic conductivity. We notice that the break observed at 873 K is accompanied at high temperature by a decreasing in the activation energy and increasing of conductivity about 100 times higher than the Ag compound. This behaviour can be strongly coupled to the structure modification. Above 873 K, the conductivity increases from $2.47 \times 10^{-5}\,\Omega^{-1}\,cm^{-1}$ at 771 K to $2 \times 10^{-4}\,\Omega^{-1}\,cm^{-1}$ at 951 K; such behaviour indicates the superionic conduction of our material.

4. Conclusion

In the present work, the single-crystal structure of the compound $LiGd(PO_3)_4$ synthesized by high temperature solid-state reaction has been determined and its ionic conduction was investigated. It crystallizes in monoclinic system with $C2/c$ space group. The three-dimensional framework of the title compound consists of twisted zig–zag chains of phosphorus tetrahedra running along the b direction, with gadolinium and lithium polyhedra connected by common corners to these chains and of coordination eight and four, respectively. The thermal evolution of $LiGd(PO_3)_4$ has been followed by TGA–DTA analysis. It shows three endothermic peaks at 602, 640 and 971 °C. The two first ones may be corresponding to structural phase transitions. The last one is due to the decomposition of the product. DSC measurements confirm the results given by DTA analysis. Since the ionic radii of Li^+ is much smaller than the Ag^+ one, it was therefore expected for Li compound to show a relatively high ionic conductivity. This phase was found to have high ionic conductivity particularly at higher temperatures. The Arrhenius plots show two changes in slope around 725 and 873 K. So, three distinct domains are observed for the variation of $\log(\sigma T)$ with temperature. The first break can be attributed to the passage of the conductivity from σac (σ along the [1 0 1] direction) to σc (σ parallel to c direction). The second one can be due to two-phase transitions. The conductivity above 873 K reaches the value of $2 \times 10^{-4}\,\Omega^{-1}\,cm^{-1}$ with an activation energy of 0.47 eV. This result is in agreement with a superionic conductor behaviour.

"Further details of the crystal structure investigation(s) can be obtained from the Fachinformationszentrum Karlsruhe, 76344 Eggenstein-Leopoldshafen, Germany, (fax: (49) 7247-808-666; e-mail: crysdata@fiz.karlsruhe.de) on quoting the depository number CSD416442."

Acknowledgments

The authors are most grateful to professor A. Driss for the X-ray data collection.

References

[1] H.G. Danielmeyer, G. Huber, W.W. Kruhler, J.F. Jesser, Appl. Phys. 2 (1973) 335–340.
[2] H.P. Weber, T.C. Damen, H.G. Danielmeyer, C.C. Tofield, Appl. Phys. Lett. 22 (1973) 534–539.
[3] S.R. Chinn, H.Y.-P. Hong, Appl. Phys. Lett. 26 (1975) 649–651.
[4] K. Otsuka, S. Miyazawa, T. Yamada, H. Iwasaki, J. Nakano, J. Appl. Phys. 48 (1977) 2099–2101.
[5] Y. Tsujimoto, Y. Fukuda, M. Fukai, J. Electrochem. Soc. 124 (1977) 553–556.
[6] H.Y.-P. Hong, Mater. Res. Bull. 10 (1975) 1105–1110.
[7] H. Koizumi, Acta Crystallogr. B 32 (1976) 266–268.
[8] I. Parreu, R. Solé, Jna. Gavaldà, J. Massons, F. Díaz, M. Aguiló, Chem. Mater. 15 (2003) 5059–5064.
[9] K. Horchani, J.C. Gâcon, M. Férid, M. Trabelsi-Ayadi, O. Krachni, G.K. Liu, Opt. Mater. 24 (2003) 169–174.
[10] K. Horchani, J.C. Gâcon, C. Dujardin, N. Garnier, C. Garapon, M. Férid, M. Trabelsi-Ayadi, J. Lumin. 94&95 (2001) 69–72.
[11] I. Parreu, R. Solé, Jna. Gavaldà, J. Massons, F. Díaz, M. Aguiló, Chem. Mater. 17 (2005) 822–828.
[12] M. Saito, T. Honma, Y. Benino, T. Fujiwara, T. Komatsu, Solid State Sci. 6 (2004) 1013–1018.
[13] H. Ettis, H. Naïli, T. Mhiri, Cryst. Growth Des. 3 (2003) 599–602.
[14] W. Rekik, H. Naïli, T. Mhiri, Acta Crystallogr. C 60 (2004) i50–i52.
[15] H. Naïli, T. Mhiri, Acta Crystallogr. E 61 (2005) i204–i207.
[16] K.K. Palkina, N.N. Chudinova, B.N. Litvin, N.V. Vinogradova, Izv. Akad. Nauk. SSSR, Neorg. Mater. 17 (1981) 1501–1503.
[17] A. Durif, Cryst. Chem. Condens. Phosphates (1995) 253–255.
[18] A.C.T. North, D.C. Philips, F.S. Mattews, Acta Crystallogr. A 39 (1968) 351–359.
[19] G.M. Sheldrich, Program for the Solution of Crystal structures, University of Götting, Germany, 1990.
[20] G.M. Sheldrich, Program for the Crystal Structure Determination, University of Götting, Germany, 1997.
[21] M.T. Averbuch-Pouchot, A. Durif, J.C. Guttel, Acta Crystallogr. B 32 (1976) 2440–2448.
[22] H.Y.-P. Hong, Mater. Res. Bull. 10 (1975) 635–640.
[23] H. Koizumi, Acta Crystallogr. B 32 (1976) 2254–2256.
[24] E.B. Zarkouna, M. Férid, A. Driss. Mat. Res. Bull. 40 (2005) 1985–1992.